A multi-fidelity approach for the evaluation of extreme wave loads using nonlinear response-conditioned waves

Athanasios Dermatis, Marine Lasbleis, Shinwoong Kim, Guillaume de Hauteclocque, Benjamin Bouscasse, Guillaume Ducrozet

Ocean Engineering 316 (2025) 119919

Contents lists available at ScienceDirect

Ocean Engineering

journal homepage: www.elsevier.com/locate/oceaneng

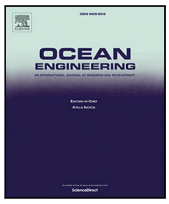

Research paper

A multi-fidelity approach for the evaluation of extreme wave loads using nonlinear response-conditioned waves

Athanasios Dermatis [a], Marine Lasbleis [b], Shinwoong Kim [a], Guillaume De Hauteclocque [b], Benjamin Bouscasse [a], Guillaume Ducrozet [a,*]

[a] Nantes Université, École Centrale Nantes, CNRS, LHEEA, UMR 6598, F-44000 Nantes, France
[b] Bureau Veritas M&O, Paris, France

ARTICLE INFO

Keywords:
Response-conditioned waves (RCW)
Most likely extreme response (MLER)
HOS-NWT
Vertical bending moment (VBM)
Extreme response prediction
Computational fluid dynamics (CFD)

ABSTRACT

In the present study, a multi-fidelity methodology based on response-conditioned waves (RCW) is demonstrated for the probabilistic assessment of wave-induced loads and responses of offshore structures. The methodology consists of two steps: (i) the RCW are determined using a surrogate response model and (ii) they are reproduced in an experimental or CFD-based numerical wave tank (NWT) to obtain the fully nonlinear response, as a high-fidelity evaluation. The main novelty of the proposed response-conditioning technique is that it uses a fully nonlinear wave solver that calculates the wave propagation inside an NWT. In this work, the extreme Vertical Bending Moment (VBM) of a zero-speed containership is investigated. It is found that the proposed approach provides nonlinear wave sequences that can be explicitly and exactly reproduced experimentally, up to very extreme sea states (H_s = 17 m, T_p = 15.5 s). Moreover, through comparison of the obtained results with an experimental Monte Carlo approach, it is shown that the overall framework can predict the short-term distribution of the VBM accurately and efficiently. Finally, given that model tests are costly and not widely accessible, the implementation of the high-fidelity response evaluation within a CFD-based NWT is also demonstrated and validated against the available experimental results.

1. Introduction

In the design of ships and offshore structures, the identification of design loads is a procedure that usually requires significant financial and temporal resources. The most prominent and reliable approach is using model tests or high-fidelity numerical tools, such as Reynolds-Averaged Navier Stokes (RANS) solvers in a Monte Carlo framework for each sea state. However, provided that the design loads are inherently rare, long irregular wave tests or simulations are required to obtain statistically converged results (van Essen et al., 2023). Furthermore, these loads also tend to be highly nonlinear, hence the use of a low-fidelity model, such as the linear potential-flow theory and Gaussian statistics, leads to significant underprediction. Attention has therefore been drawn towards alternative approaches to overcome this limitation (van Essen and Seyffert, 2023). Among these, the present paper focuses on the response-conditioned waves (RCW) approach for design load analysis.

Tromans et al. (1991) introduced the concept of conditional waves with the "New Wave" model, which uses a conditional mean process to express the most probable wave shape around a crest, assuming that the wave elevation is a zero-mean stationary Gaussian process. Along the same lines, the most likely wave (MLW) method (Friis-Hansen and Nielsen, 1995) determines the crest-conditional wave profile with the concurrent conditioning of the crest amplitude and the random instantaneous frequency of the wave. The aforementioned methods are equivalent when the conditional frequency is equal to the mean wave frequency $\omega_1 = m_1/m_0$, where m_i is the ith moment of the wave spectrum. Adegeest et al. (1998) introduced the most likely extreme response (MLER) method, which uses a linear transfer function of the structure's response to determine the wave sequence that excites a given response amplitude. Similar to MLW, the most likely response wave (MLRW) (Dietz, 2004) determines an RCW based on a concurrent conditioning of the response amplitude and the instantaneous frequency. In the same study, the conditional random response wave (CRRW) was also developed, which consists of the MLRW embedded in a random background wave elevation. Moreover, the design loads generator (DLG) method (Alford, 2008; Kim, 2012; Seyffert, 2018) determines the Gaussian wave events that will excite a specific response, based on their non-uniform phase distribution.

However, considering linear waves and a linear transfer function limits the applicability of these approaches to configurations where

* Corresponding author.
E-mail address: guillaume.ducrozet@ec-nantes.fr (G. Ducrozet).

https://doi.org/10.1016/j.oceaneng.2024.119919
Received 12 September 2024; Received in revised form 14 November 2024; Accepted 24 November 2024

Table 1
Overview of several RCW approaches.

		Responses	
		Linear	Nonlinear
Waves	Linear	Adegeest et al. (1998) Dietz (2004) Alford (2008)	Jensen and Capul (2006) Seyffert (2018) Lim and Kim (2018)
	Nonlinear	–	Ghadirian and Bredmose (2019) Takami et al. (2023)

extreme linear responses do not largely deviate from the corresponding nonlinear responses. To this end, in Lim and Kim (2018), the MLER method was extended to the second order using a Volterra system representation and the Quadratic Transfer Function (QTF) to account for the pure slow-drift motions of a semi-submersible. In a more general context, the First Order Reliability Method (FORM) (Der Kiureghian, 2000) uses a limit state function for the response-conditioning and allows for the use of response models of any degree of nonlinearity. Jensen and Capul (2006) applied the FORM for the prediction of wave loads and extracted an explicit expression of the mean up-crossing rate as a function of the reliability index. The method has been extensively studied for complex scenarios, such as the wave-induced loads on flexible hulls (Jensen et al., 2014), parametric rolling (Jensen et al., 2017), and combined wind and wave loading (Jensen et al., 2011). Takami et al. (2023) used a nonlinear Higher-Order Spectral (HOS) wave model, coupled with FORM for the prediction of extreme wave-induced loads and motions. In particular, numerical investigation was carried out for the analysis of wave crest, vertical bending moment (VBM) and roll motion distribution in beam seas. Comparison between the results obtained by linear and nonlinear incident waves showed that wave nonlinearity has a significant influence on the prediction of the tail values of the distribution. Nevertheless, in the applications of the FORM mentioned above, the extreme response predictions are performed using the up-crossing rate formulation of Jensen and Capul (2006) and they are not applied in a multi-fidelity context.

Moreover, despite the notable progress in the identification procedures for the RCW episodes, their flawless implementation in experimental (EWT) or numerical wave tanks (NWT) is still challenging. The majority of these response-conditioning techniques are based on linear wave theory and therefore provide unrealistic wave episodes for severe sea states. Hence, when implemented experimentally, nonlinear wave–wave interactions during the propagation of those wave sequences will result in a wave episode whose shape deviates from the target RCW (Drummen et al., 2009; Quon et al., 2016; Hann et al., 2018). Such differences in the incident waves are expected to introduce considerable uncertainties in the assessment of the fully nonlinear responses. To overcome this issue, Ghadirian and Bredmose (2019) coupled the FORM with fully nonlinear wave kinematics using the OceanWave3D model (Engsig-Karup et al., 2009). The experimentally averaged force on a monopile and respective wave elevation showed better agreement with the fully nonlinear wave case than with the first or second order. Kim et al. (2022) coupled the nonlinear wave solver HOS-NWT (Ducrozet et al., 2012) with FORM to predict the wave crest distribution. The wave episodes were generated very accurately in the experiments and the crest height distribution was predicted very efficiently. An overall non-exhaustive mapping of the different RCW techniques, based on their assumptions about the linearity of the incident waves, as well as the responses of the structure can be found in Table 1.

As it has been briefly discussed so far and will be more extensively analysed in Section 3, using such RCWs as design waves usually requires a high-fidelity nonlinear wave–structure interaction model, which for most practical applications consists of model tests or CFD. Within these environments, waves are generated and propagated in EWTs or NWTs and the use of linear wave models in the response-conditioning procedure poses several limitations to that approach. Therefore, the motivation for this study is to introduce a response-conditioning method, which considers the nonlinear propagation of the waves in an NWT and can determine nonlinear design wave episodes. This will not only facilitate the reproduction of the RCW in the wave tanks but also allow the investigation of more complex responses where the wave nonlinearity is significant (van Essen and Seyffert, 2023). The proposed approach is integrated into a multi-fidelity methodology which consists of two steps and re-evaluates a preliminary surrogate response distribution, according to the high-fidelity response of the structure to single-wave episodes. As a first step, an optimization procedure, similar to the FORM, is used to determine the RCW, coupled with the fully nonlinear wave solver HOS-NWT (Ducrozet et al., 2012). Therefore, the second step, which consists of the reproduction of those wave episodes with high-fidelity tools, can be easily implemented and the fully nonlinear response to those RCW can be obtained. The objective of this methodology is to replace time-consuming Monte Carlo tests in irregular waves with short-duration experiments or numerical simulations in RCW, allowing the swift evaluation of the short-term extreme responses, across a wide range of sea states. By achieving this, the method potentially enables accurate and efficient calculation of long-term design loads, even at early design stages, where introducing high-fidelity tools would be otherwise cost-prohibitive.

In the present paper, a case study is performed using a rigid 6750-TEU containership, where the response of interest is the VBM at near amidships. A surrogate model is constructed using the nonlinear waves at the structure's location and the linear response amplitude operator (RAO) of the VBM. The Rayleigh distribution is obtained using the variance of the linear VBM response spectrum and for certain levels of exceedance probability, the corresponding VBM values are extracted. Following, these target VBM values are used in the conditioning process, to determine appropriate wave episodes for both hogging and sagging conditions and within five sea states. Through the experiments, the fully nonlinear VBM response values that correspond to the predefined POE levels are obtained and the results are compared with a Monte Carlo approach in irregular waves. Finally, provided that CFD is the most suitable approach for practical applications, the high-fidelity evaluation of the response distribution using CFD instead of experiments is also investigated. The article begins with an overview in Section 2 of the different approaches that are used for the probabilistic assessment of the extreme responses of offshore structures. The multi-fidelity framework along with the proposed response-conditioning approach are detailed in Section 3, followed by a description of the experimental setup, environmental conditions, and test cases in Section 4. In Section 5, the methodology is verified experimentally, while it is also demonstrated that CFD can be used as a high-fidelity model in practical applications. Finally, the conclusions of the present study are drawn in Section 6.

2. Extreme response statistics

In this section, several existing methodologies for the probabilistic assessment of the fully nonlinear wave-induced response of offshore structures are discussed. The Monte Carlo method is first outlined, along with several strategies that allow the optimization of the required test duration and number of seeds. Following, the general context and principles of the multi-fidelity approach for efficient estimation of the extreme wave-induced response statistics is described and two examples of the application of this framework are given. Finally, the focus is drawn on the design wave approach, which is also the subject of the present study.

2.1. Monte Carlo approach

To evaluate the exact wave-induced response distribution of marine structures, the Monte Carlo approach in irregular waves is considered as the reference procedure. Through up-crossing analysis of the response time series, the maxima and minima of each cycle are determined, sorted, and associated with the empirical exceedance probability $P_c = 1 - \frac{i}{N+1}$, where N is the total number of events and i is the index of the sorted events. Multiple realizations of the sea state considered are necessary to obtain statistically converged results up to the desired exceedance probability level. The test duration, as well as the number of those realizations, is usually defined by appropriate guidelines and varies depending on the structure under consideration (van Essen et al., 2023).

This method can be optimized to a great extent and with negligible loss of accuracy through efficient sample selection (Mohamad and Sapsis, 2018), as well as through the increased design sea-state (IDSS) approach (Derbanne et al., 2012). The concept of the IDSS is the artificial increase of the significant wave height, to observe occurrences of a given response level more frequently. According to Kim et al. (2024a), a speed-up of 8 times with 0.1% error can be achieved, even for moderate/extreme sea states. Similar to the IDSS, the scaling properties of the FORM reliability index can numerically predict the extreme response distribution (Jensen, 2011). Moreover, when low probability levels are sought, statistical extrapolation from a limited dataset of shorter duration is possible instead of using the empirical distribution (Song et al., 2019). However, fitting a distribution to the limited dataset might potentially introduce bias in the prediction.

2.2. Multi-fidelity approaches

The methodologies presented below are grouped according to their principal common feature, which is the combined use of response models of different fidelity levels to evaluate the response statistics. More specifically, instead of conducting the full Monte Carlo procedure using experiments or CFD, only selected events are treated with high-fidelity tools. The identification of the critical events is made based on a surrogate model of low or medium fidelity, which needs to be efficient and precise enough for the driving mechanism of the extreme events to be captured. For most wave-induced responses, the linear response obtained by the application of the RAO to the wave elevation is an adequate surrogate. However, for more complex scenarios, time-domain models that include several nonlinearities can be a step towards a more refined model. Under these terms, the linear and nonlinear extremes will occur in similar time instants but will differ in magnitude and therefore the underlying critical wave episodes can be identified and extracted.

2.2.1. Wave screening

The concept of this approach is to use a surrogate response model to perform the Monte Carlo in irregular waves, with reasonable computational effort. Based on the assumption about the coincidence of the linear and nonlinear extreme events in time, the wave episodes that are expected to induce large responses are identified and then reproduced through a high-fidelity model, to obtain the fully nonlinear responses. Eventually, the low-fidelity statistics are combined with the results from the high-fidelity analysis, to obtain an estimation of the response distribution. This approach has been introduced in Torhaug (1996) where the linear response was used for the screening of the waves and weakly nonlinear seakeeping tools were used for the nonlinear evaluation of wave loads. In van Essen et al. (2021), both potential flow solvers and CFD solvers on coarse meshes have been used for the screening, while it was also found that screening methods can potentially reduce the necessary time of experiments or refined numerical simulations up to 90%, compared to the full Monte Carlo approach.

2.2.2. Design waves

The term design waves is used here to describe the methodologies according to which a single wave episode is used as an equivalent to the irregular sea state. In general, a distinction is made between the case of regular wave episodes, commonly known as equivalent design waves (EDW), and irregular design wave episodes, also referred to as response-conditioned waves (RCW). Classification societies have extensively used the former in their rules and guidelines due to their simplicity; however, they are known to provide less accurate results compared to the latter (de Hauteclocque et al., 2012). For regular waves, the standard practice is to set the frequency equal to the peak frequency of the linear response spectrum and determine the wave height through the target response divided by the value of the RAO for the peak frequency. For irregular waves, the design wave corresponds to the conditional wave episode determined through one of the methods discussed in the introduction. These wave episodes are implemented in a multi-fidelity framework within which the surrogate response model is used to back-calculate a short wave episode for any response level, which is expected to induce this load or motion at a given time instant. Lastly, these wave sequences can be reproduced with high-fidelity means to get a fully nonlinear response. The main advantage of this method is that the duration of the tests does not depend on the level of the response. Therefore, for very extreme responses, where the rare occurrence of the underlying wave episodes would necessitate a large exposure time and a large number of realizations, the EDW or RCW methods solely require the implementation of several wave episodes. In particular, Brown et al. (2023) found that the design wave approach, was 43 times more efficient than Monte Carlo when a single wave episode was investigated. Under these terms, especially for very low probability levels, for which the irregular wave test duration would increase significantly, the design wave approach can directly estimate the fully nonlinear response with only 1 min of model tests or high-fidelity numerical simulations.

3. Design wave methodology

As mentioned in the introduction and further analysed in Section 2, a multi-fidelity approach based on design waves is used in this paper for the prediction of the extreme VBM responses of a containership. This approach consists of two steps. The first entails the determination of the design wave through a response-conditioning procedure and by using a surrogate model. The second step involves the evaluation of the fully nonlinear response of the structure to those design wave episodes, through a high-fidelity model.

To predict a particular response distribution, each RCW should correspond to a level of POE. To this end, a preliminary response distribution is obtained through the surrogate model, either through an explicit expression or through efficient Monte Carlo simulations. Following, for certain levels of probability, the equivalent responses are extracted and used for the response-conditioning. It is recalled here that this surrogate needs to capture the driving mechanisms that excite the extreme responses. For the case study addressed in this paper, the response of interest is the VBM of a non-slender body, driven by wave phenomena. Thus, the linear diffraction/radiation theory is an adequate surrogate model and an RAO-based model is constructed, while the Rayleigh distribution serves as the preliminary distribution.

The first of the following subsections includes a description of all the different aspects of the response-conditioning procedure. It starts with the motivation of using a nonlinear wave model that propagates the waves in NWT, along with its formulation. The adopted surrogate response model is introduced, together with the procedure that is implemented to obtain the response-conditioned waves. The second subsection gives a brief introduction to the implementation of the calculated RCW episodes in a high-fidelity tool, which is further analysed for the present setup in Section 4.

3.1. Higher order spectral response-conditioned waves (HOS-RCW)

The majority of existing RCW methods assume a linear wave field to obtain an explicit formula for the wave elevation. The closed-form expression of the wave elevation and the response makes use only of the spectral information and the response transfer function and thus it can be implemented to explicitly derive the appropriate design wave episodes. Because of their practicality, linear response-conditioning techniques have been used extensively in the literature for various types of structures and responses (Quon et al., 2016; Ripe and Lande-Sundall, 2023; Drummen et al., 2009; Brown et al., 2023; Jin et al., 2022). However, when used in a multi-fidelity approach, within which episodes are reproduced in model tests or CFD, there are several limitations. More specifically, nonlinear wave–wave interactions during the propagation of the wave sequence from the wave generation up to the location of the structure will alter the phases of the wave packet and its shape will be different from the theoretical profile (Fernández et al., 2014). As a result, the wave encountered by the structure will deviate from the determined RCW and uncertainties will be introduced in the methodology (Drummen et al., 2009). This problem is expected to be intensified when considering constrained wave episodes, where the RCW will also interact with the background irregular wave (Hann et al., 2018). On top of that, when it comes to wave impact-related problems, such as green water on deck or slamming, the loads highly depend on the incident wave crest height and steepness. Thus, including wave nonlinearity in the surrogate model might be crucial for this type of application, as discussed in van Essen and Seyffert (2023).

Frequency domain phase and amplitude correction have been applied previously (Schmittner et al., 2009; Fernández et al., 2014) to improve the generation of the wave episodes, as demonstrated in Tosdevin et al. (2022) and Takami et al. (2020). However, the waves obtained experimentally through this approach still present some discrepancies with the target wave profiles. Besides, the target RCWs remain linear, according to the underlying response-conditioning technique and they are not representative of realistic environmental conditions. Therefore, the present study aims to treat this problem by introducing a response-conditioning technique that provides nonlinear wave episodes. Those RCW not only can be flawlessly reproduced in experiments and CFD as shown in Sections 5.1.1 and 5.2, but also retain their nonlinearity, since a nonlinear NWT is incorporated in the surrogate model.

3.1.1. Nonlinear numerical wave tank

The Higher-Order Spectral (HOS) method (Dommermuth and Yue, 1987; West et al., 1987) is an efficient way of solving numerically the nonlinear wave propagation in an open fluid domain, using potential flow theory. The method has been further developed to account for the generation and propagation of waves in a numerical wave tank by Ducrozet et al. (2012). In a complete analogy to all the features of an experimental wave tank, in the HOS-NWT approach: i) the waves are generated through the motion of a numerical wavemaker, ii) the sidewalls are fully reflective and iii) an absorbing beach is located opposite to the wavemaker to prevent the reflections from the opposite wall. The accuracy and efficiency of the open-source HOS-NWT solver have been validated through several studies on various configurations (Aliyar et al., 2022; Ducrozet et al., 2016; Seiffert et al., 2017) and is therefore adopted in the present approach.

3.1.2. Surrogate response model

A schematic depiction of the aforementioned numerical wave tank is demonstrated in Fig. 1. The waves at the location of the structure x_0 are controlled by the numerical wavemaker motion, which is assumed to be a zero-mean Gaussian process and serves as the input of the FORM-based procedure (see Section 3.1.3).

$$\begin{aligned} X_{wm}(t) &= \sum_{i=1}^{N} \frac{\alpha_i}{\mathrm{TF}_i} \cos(\omega_i t + \epsilon_i) \\ &= \sum_{i=1}^{N} (u_i c_i(x,t) + \bar{u}_i \bar{c}_i(x,t)) \end{aligned} \tag{1}$$

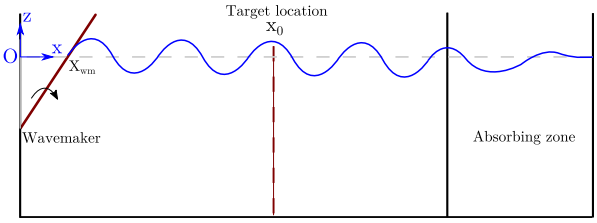

Fig. 1. Numerical wave tank configuration.

where N is the total number of wave components generated at the wavemaker location, ω_i is the frequency of the ith components and $\alpha_i = \sqrt{2S_\eta(\omega_i)d\omega}$ is their amplitude defined from the target wave spectrum $S_\eta(\omega_i)$. Moreover, TF_i is the modulus of the wavemaker transfer function and ϵ_i is the phase. Finally, u_i, $\bar{u}_i$ are uncorrelated standard normal variables that serve as the unknown variables for this problem, while the deterministic functions $c_i(x,t)$ and $\bar{c}_i(x,t)$ follow

$$\begin{aligned} c_i(x,t) &= \sigma_i^{wm} \cos(\omega_i t - k_i x) \\ \bar{c}_i(x,t) &= -\sigma_i^{wm} \sin(\omega_i t - k_i x) \\ \left(\sigma_i^{wm}\right)^2 &= \frac{S_\eta(\omega_i)}{\mathrm{TF}_i^2} d\omega_i \end{aligned} \tag{2}$$

where $(\sigma_i^{wm})^2$ denotes the variance of the wavemaker motion, while the amplitudes and phases are

$$\frac{\alpha_i}{\mathrm{TF}_i} = \sigma_i^{wm} \sqrt{u_i^2 + \bar{u}_i^2} \qquad \epsilon_i = \tan^{-1}\left(\frac{\bar{u}_i}{u_i}\right) \tag{3}$$

Using the wavemaker motion described above, HOS-NWT solves for the nonlinear wave propagation inside the wave tank and outputs the nonlinear free-surface elevation at the structure's location $\eta_{HOS}(x_0,t)$. Under these terms, the surrogate response of interest can be evaluated through the Fourier Transform of this wave elevation, application of a transfer function and Inverse Fourier Transform to transit back in the time domain as shown below.

$$\eta_{HOS}(x_0,t) = \sum_{i=1}^{N} A_i e^{-\mathrm{i}\omega_i t} \tag{4}$$

Then the surrogate response will follow,

$$\chi(x_0,t) = \sum_{i=1}^{N} RAO(\omega_i) A_i e^{\mathrm{i}\omega_i t} \tag{5}$$

where A_i are the complex Fourier coefficients of the wave amplitude. Through this surrogate model, all the frequency components A_i are treated as free waves and therefore the resulting response is linear. However, at the location of the structure x_0, the incident wave field has the correct phase, due to the nonlinear propagation, solved by HOS-NWT.

3.1.3. Response-conditioning procedure

A response-conditioning procedure similar to the one used in the First Order Reliability Method (FORM) is adopted to calculate the RCW episodes. In both approaches, the point on the limit state function of minimum distance from the origin is determined. However, the distinctive feature between the approach presented here and the FORM is that after finding this point, there is no assumption about the order of the limit state function. Instead, the point is recovered and the corresponding wave episode realization is sought as the RCW. More specifically, a surrogate model is used for the response of interest, as well as a predetermined threshold χ_{tar} to define the limit state function, as

$$G(\mathbf{u}) = \chi_{tar} - \chi(x_0, t_0 | \mathbf{u}) = 0 \tag{6}$$

where $\mathbf{u}$ corresponds to a vector of uncorrelated normal distributed variables, $\{u_i, \bar{u}_i\} = \{u_1, \bar{u}_1, u_2, \bar{u}_2, \ldots, u_N, \bar{u}_N\}$. Different realizations of those variables will yield different outcomes of the wavemaker motion

(Eq. (1)) and through the surrogate model will result in different responses within the limit state function. Since the limit state function is defined in the standard normal space, the point $\mathbf{u}^*$ with the shortest distance to the origin corresponds to the realization with the highest probability of occurrence and is therefore denoted as the most probable point (MPP). Therefore, the following optimization problem is constructed, the solution of which will provide the MPP, which for the formulated wave–structure interaction problem will correspond to the RCW,

$$\min \sqrt{\sum_{i=1}^{N}(u_i^2+\bar{u}_i^2)} \quad \text{subject to} \quad G(\mathbf{u})=0 \tag{7}$$

To this end, an iterative algorithm known as Modified Hasofer and Lind with Goldstein–Armijo rule (MHLGA) (Santos et al., 2012; Kim et al., 2022) is employed in the present study, to determine the MPP. The initial point of the optimization is set as the wave episode calculated by the MLER approach (Adegeest et al., 1998). Upon determination of the MPP, the Gaussian wavemaker motion can be determined through the same equation and the wave episode can be reproduced in a very straightforward manner in a high-fidelity environment. It shall be noted that in this approach, the wave elevation, as well as the response that is included in the limit state function, are not explicitly related to the wavemaker motion. For this reason, HOS-NWT simulations need to be performed during each iteration of the MHLGA algorithm, which might significantly increase the computational time if the solver parameters are not chosen carefully. The total number of HOS-NWT simulations varies depending on the required iterations for the method to converge. As a general rule, 2N simulations are performed during each iteration, equal to the size of the $\mathbf{u}$ vector.

3.2. High-fidelity nonlinear response evaluation

The second step of the present methodology consists of the reproduction of the HOS-RCW in a high-fidelity environment. The output of the procedure described in the previous subsection is the motion of a numerical wavemaker $X_{wm}(t)$ given by Eq. (1). Therefore, the reproduction of the RCW in an EWT is explicit, while in a CFD-based NWT, the HOS-NWT solver can be coupled with the viscous solver through a domain decomposition approach as shown in Aliyar et al. (2022). An overall schematic depiction of the multi-fidelity design wave methodology is shown in Fig. 2. The left side of this Figure corresponds to a flowchart of the general two-step methodology and the right side to an illustration of the nonlinear response evaluation through the use of design waves.

4. High-fidelity tools

For the evaluation of the fully nonlinear loads on the structure during the second step of the methodology, two high-fidelity models are investigated here, namely experiments and CFD simulations. First, the description of the experimental setup is provided along with the main particulars of the containership model. Moreover, the basic aspects of the numerical solver and the construction of the CFD-based NWT and meshing strategy are outlined. Finally, the test conditions are presented both in terms of RCW, as well as irregular waves used for the verification of the methodology.

4.1. Experimental setup

Experiments were conducted in the Ocean Engineering Wave Tank of École Centrale Nantes for a 6750-TEU containership under a scale of 1/65. The model is identical to the one used in Bouscasse et al. (2022), Kim et al. (2023b) and Kim et al. (2024a), while its dimensions can be found in Table 2. It is divided into 9 segments, the intersections of which ensure the rigidity of the structure. Under these terms, it is possible to isolate the nonlinear effects attributed to the geometry of the hull and the incident waves from the hydroelastic effects. An ATI sensor is installed near amidships, where the maximum bending moment is expected to occur and measures directly the 6-DOF internal loads (Fig. 3).

Table 2
Principal dimensions of the 6750-TEU containership.

	Full scale	Model scale
Scale	1/1	1/65
LBP (m)	286.6	4.409
Breadth (m)	40	0.615
Draft (m)	11.98	0.188
Displacement (kg)	85663776	311.93
KM (m)	18.662	0.287
GM (m)	2.10	0.032
KG (m)	16.562	0.257
LCG from AP (m)	139.56	2.147
kxx (m)	14.4	0.222
kyy (m)	71.5	1.109
kzz (m)	71.4	1.106

The experimental apparatus is presented in Fig. 4, where the body-fixed reference frame is defined with the origin O_b amidships and at the waterline. Eight resistive wave gauges (WG) are installed in different locations in the wave tank for the measurement of the free-surface elevation. The monitoring of the incident wave field at the location of the structure is performed through WG2, which is aligned with the ATI sensor in calm water. A more detailed description of the experimental setup and measuring devices can be found in Bouscasse et al. (2022).

4.2. Numerical setup

The RANS equations are solved with the in-house code foamStar, using the Finite-Volume library and utilities from OpenFOAM (Jasak, 1996). foamStar is a Volume of Fluid (VoF) solver (Hirt and Nichols, 1981) co-developed by Bureau Veritas and Centrale Nantes and based on the interFoam solver. It contains a library of validated utilities for wave generation (Kim et al., 2024b) and hydro-elastic and rigid fluid–structure interactions (Seng et al., 2014; Aliyar et al., 2022). The HOS-NWT wave profiles are generated through dedicated relaxation zones, with a grid interpolation, from the HOS-NWT domain to the CFD domain (Kim et al., 2024b).

In the case of RCW, the setup is mostly governed by the short duration and short length span of the waves of interest. This allows for a significant decrease in the domain size compared to regular or irregular waves. For this particular case, the reflected waves do not have the time to reach the boundary of the domain before the end of the computation and thus, a relatively short domain with reduced relaxation zones can be used (Aliyar et al., 2022). OpenFOAM tools were used for constructing the mesh and more specifically, a background mesh was built with wave amplitude-dependent refinement around the free surface and the ship position. In the present study, all the RCWs considered within a sea state have a similar zero-crossing period, while their amplitudes vary from $1H_s$ to $1.6H_s$. Therefore, the same mesh and free-surface zone was used for all wave episodes of the same sea state, on the condition that there is an adequate number of cells in the vertical direction. Finally, the ship boundary was created with SnappyHexMesh and the numerical domain is presented in Fig. 5. Moreover, given that RCW are single wave packets starting from calm water conditions, only a few seconds before the ship encounters the incident waves are computed in the numerical simulations. Under these terms, the numerical setup can be further optimized compared to the simulation of long time series of irregular waves, since the total duration of the computation can be further reduced. Therefore, it is demonstrated here that due to the nature of the RCW, significant efficiency can be gained both in terms

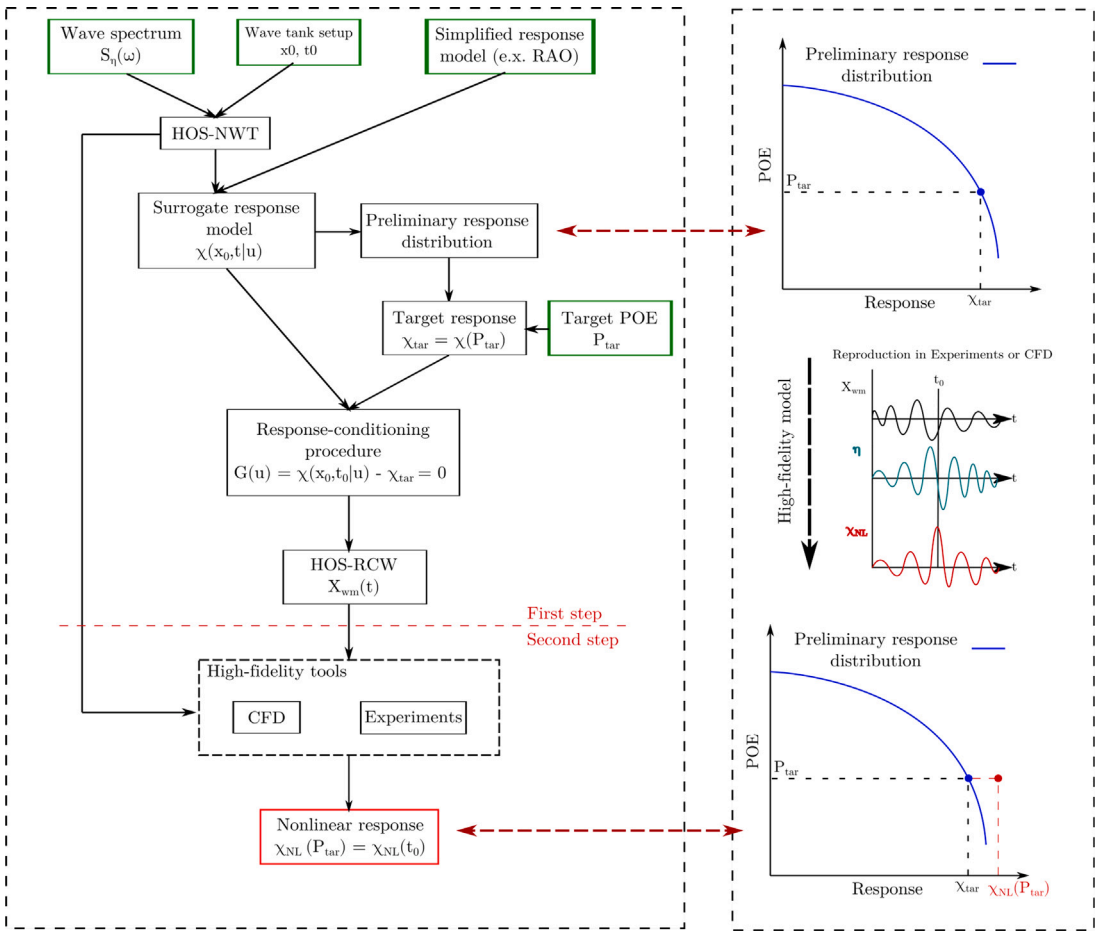

Fig. 2. Flowchart of the design wave methodology.

Fig. 3. 6750-TEU containership model.

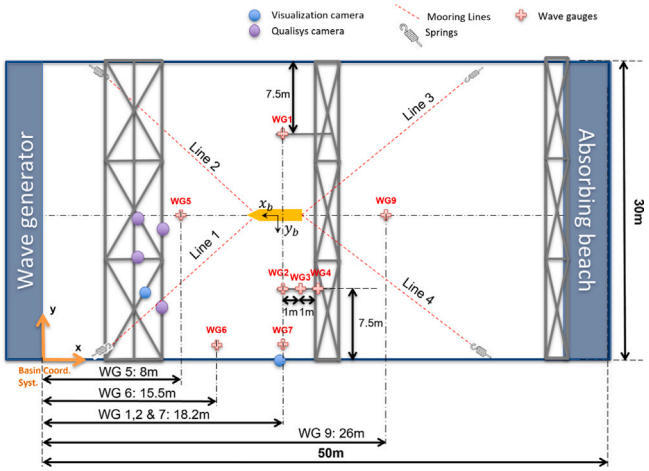

Fig. 4. Experimental setting for heading wave condition.

of domain size and simulation time. In addition, provided that during the RCW simulations no breaking is observed, no turbulence model is employed.

Finally, to validate the wave propagation in the CFD-based NWT, the same RCW is required to be simulated in a two-dimensional setup, without the presence of the body. To this end, two-dimensional slices are extracted during the mesh construction process, after all the refinement zones are imposed and before using snappyHexMesh.

4.3. Irregular wave tests

Five sea states defined by the JONSWAP spectrum are considered in this study, as shown in Table 3. Irregular wave tests were conducted experimentally to obtain the reference distribution through a Monte Carlo approach. To obtain statistically converged results, each sea state was repeated several times and with different realizations of wave phases. The duration of each test corresponds to around 20 min in model scale (2h40 full scale), from which one minute from the beginning and the end of the test were excluded from the analysis, to eliminate transient phenomena. The results of the experimental study on irregular waves along with the relevant statistical analysis can be found in Kim et al. (2024a).

4.4. Response-conditioned wave tests

Regarding the experimental RCW analysis, several target VBM values were chosen for each sea state according to the Rayleigh distribution. In total, eight values per sea state were considered, consisting of four cases for the hogging condition and four for the sagging condition,

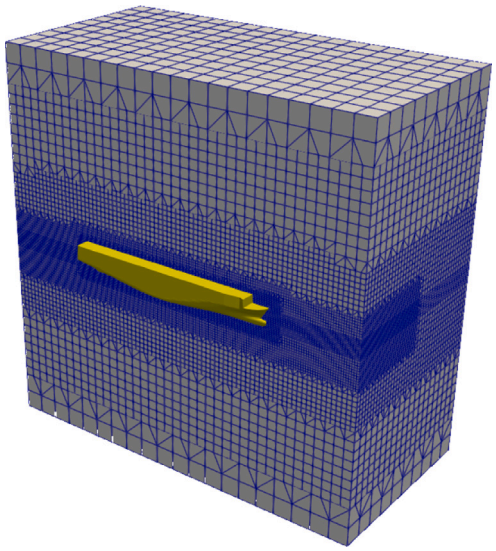

Fig. 5. Computational domain for RCW simulations.

Table 3
Description of 5 different environmental conditions (full scale).

Case	H_s (m)	T_p (s)	γ	Seeds	Nb. of waves
SS6	6	12.25	1	8	7600
SS8	8.3	14	1.5	12	9800
SS10	10	14	1.5	10	8000
SS12	12	14	1.5	8	6200
SS17	17	15.5	2.6	34	23 000

Table 4
VBM target values for RCW analysis in model scale (Nm).

Index	POE	SS6	SS8	SS10	SS12	SS17
1	$\mathbf{10^{-1}}$	61.8	98.7	118.9	142.7	207.8
2	$\mathbf{10^{-2}}$	87.4	139.6	168.1	201.8	293.9
3	$\mathbf{5{\cdot}10^{-3}}$	93.8	149.7	180.3	216.4	315.2
4	$\mathbf{10^{-3}}$	107.1	170.9	205.9	247.1	359.9

based on their levels of exceedance probability, as shown in Table 4. Provided that the Rayleigh distribution is symmetric for hogging and sagging conditions, the target values for the sagging cases were set as -VBM_{tar} and the RCW episodes were extracted for those response levels. Furthermore, all calculated RCW were designed to induce the maximum response at $t_0 = 45$ s and at $x_0 = 18.2$ m, which coincides with the location of the 6-DOF load sensor (ATI). For the numerical investigation, only SS10 was considered in both hogging and sagging conditions.

5. Results and discussion

In the present section, the application of the proposed methodology is demonstrated for an experimental wave tank, as well as through high-fidelity CFD simulations. The objective of the former part is to verify that the methodology provides an accurate and reliable estimation of the fully nonlinear response distribution and compare it against a reference experimental Monte Carlo distribution based on irregular waves. On the other hand, the objective of the latter part is to investigate the applicability of the methodology in a purely numerical environment. To this end, upon validating the capacity of a CFD solver to accurately capture the VBM of the containership, the second step of the methodology is applied in a CFD-based NWT and the VBM response distribution is constructed using the peaks from the individual RCW simulations.

5.1. Experimental investigation of design wave methodology

5.1.1. Assessment of nonlinear RCW reproducibility

The first step for the verification of the methodology is to assess the quality of the reproduced wave episodes. Extensive repeatability tests for the exact same setup under steep regular waves were performed by Bouscasse et al. (2022). Moreover, the experimentally measured wave elevation through WG2 is compared against the respective elevation computed from HOS-NWT and this comparison is illustrated in Figs. 6 and 7 for the mildest and the most severe sea state (SS6 and SS17 respectively). For the other sea states the relevant figures are omitted due to similar trends and limited additional insight, but are available upon request. In each figure, the top row corresponds to the hogging results in ascending order of target VBM values, while the bottom row corresponds to the sagging results. The RCW scenarios are named according to the sea state and an index that corresponds to the POE level, as shown in Table 4. All wave episodes derived by the HOS-RCW method are reproduced with excellent accuracy and are equivalent to the numerically determined wave elevation, in contrast with what would be expected from linear response-conditioned waves (Drummen et al., 2009; Quon et al., 2016).

The second aspect that needs to be verified is that the surrogate model is fit for its purpose. It is recalled here that the surrogate model should be able to identify the nonlinear maxima. In other words, the linear and nonlinear extreme events should differ in terms of amplitude and approximately coincide in time. To this end, the experimentally measured wave-induced VBM is compared with the surrogate response in Figs. 8–9 for SS6 and SS17 respectively. Through this comparison, it is verified that the experimental VBM indeed coincide in time with the linear response, while the nonlinearities in hogging conditions reduce the maximum response and they are enhancing the sagging. Therefore, the results confirm that the surrogate model based on a combination of nonlinear wave propagation and a linear response is a suitable surrogate for the response-conditioning.

5.1.2. Extreme wave and response profiles

At this point, it has been confirmed that the reproduced waves and the surrogate model from the first step of the methodology provide reliable input for the second step of the high-fidelity evaluation. Hence, the analysis proceeds with a more in-depth investigation regarding the likelihood of the occurrence of those fully nonlinear wave episodes and respective responses. More specifically, the free-surface elevation and VBM time series for the individual HOS-RCW episodes are compared here against similar events from the Monte-Carlo irregular tests. For each RCW scenario, irregular wave instances are extracted, during which a VBM response of ±5 % magnitude was recorded. It should be emphasized that strictly speaking, the ensemble of all these similar events will not correspond to the most probable realization. However, it provides a good estimate for that purpose.

The comparisons between the RCW and the irregular wave events of analogous response levels are presented in Figs. 10–13 for SS6 and SS17. The RCW scenarios are presented in ascending order of maximum VBM magnitude, with the wave elevation in the top row and the VBM response in the bottom row. Regarding the wave elevation, the RCW follows the general trend of the average irregular wave profile, especially before the occurrence of the peak VBM response. Past this point, the RCW free-surface elevation deviates from the average and more specifically it appears to have deeper troughs and higher crests. On the contrary, the comparison between RCW-induced VBM with the average profile of the irregular wave events shows an even better agreement throughout the whole time history. More specifically, for the mild and moderate sea states, the two response profiles nearly overlap, despite the slight differences in the underlying wave elevation. As the sea state severity increases, larger deviations appear gradually and especially for the hogging case, in the neighbouring troughs of the maximum VBM. Overall, the results indicate that the high-fidelity evaluation of the waves and responses derived by the HOS-RCW methodology provides results that are very close to the ensemble of the irregular wave events and might be seen as the most probable outcomes.

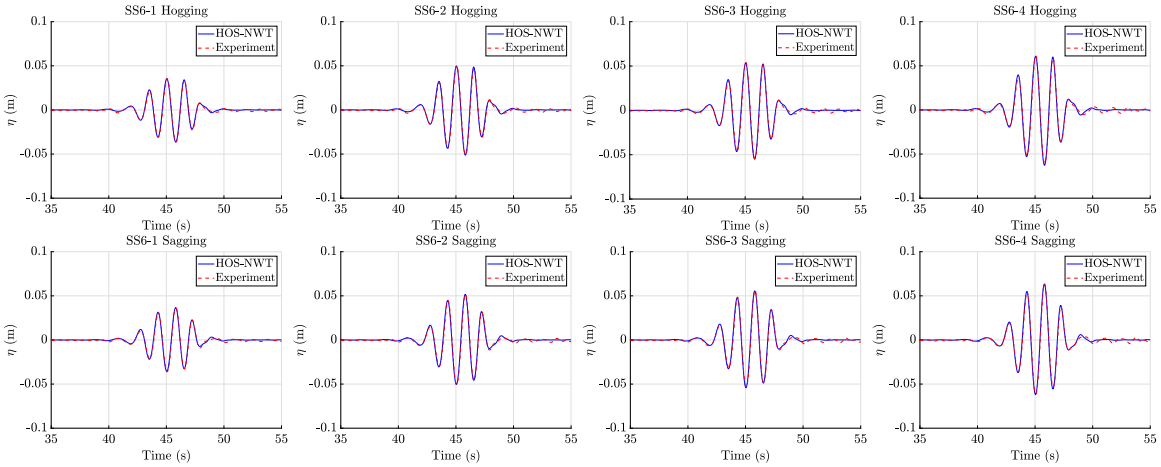

Fig. 6. Experimentally reproduced wave profiles for hogging (top row) and sagging (bottom row) for SS6.

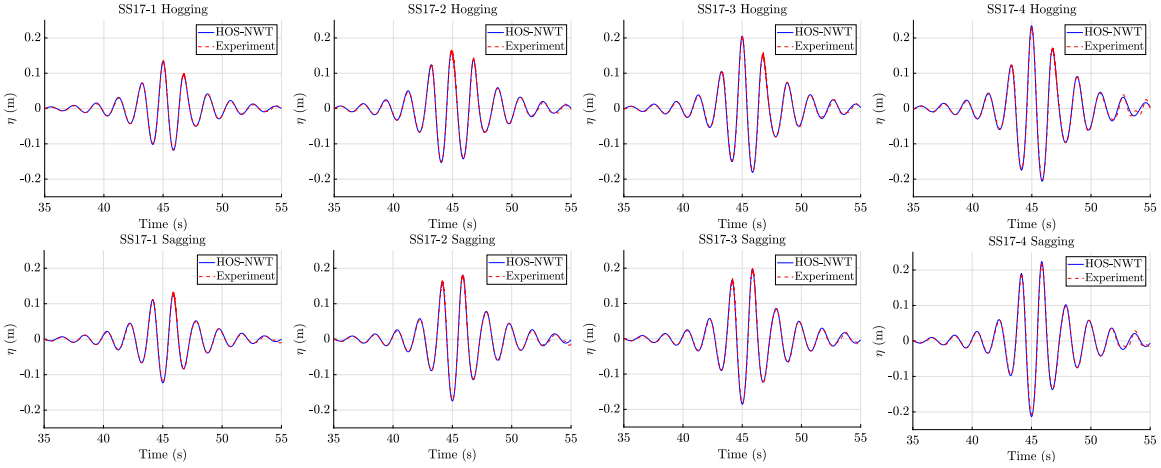

Fig. 7. Experimentally reproduced wave profiles for hogging (top row) and sagging (bottom row) for SS17.

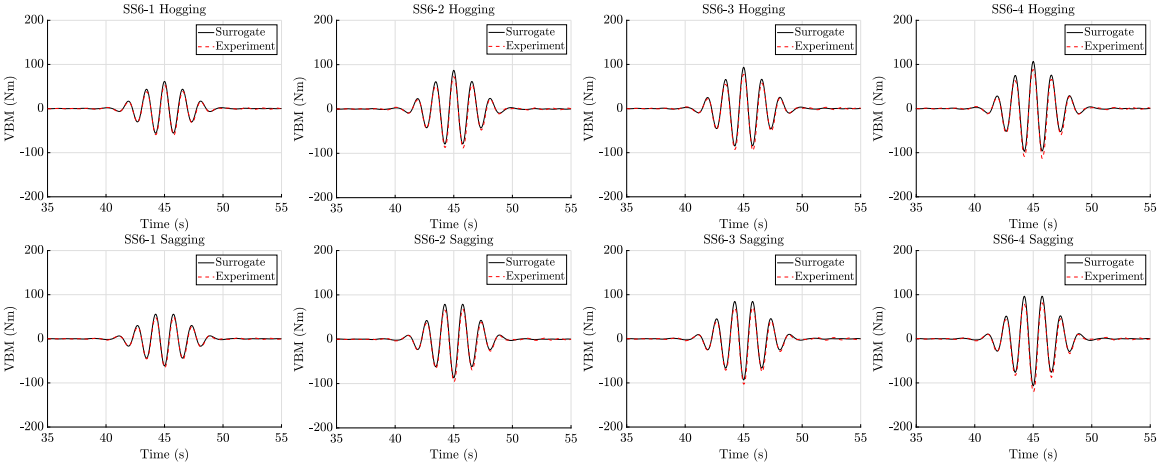

Fig. 8. Experimentally measured VBM responses for hogging (top row) and sagging (bottom row) for SS6.

5.1.3. Extreme short-term response prediction

As mentioned in Section 4 irregular wave tests were performed for each sea state and the relevant results can be found in Kim et al. (2024a). By applying zero-crossing analysis on the irregular VBM time series and sorting the local maxima and minima in ascending order of magnitude, reference distributions can be constructed according to the Monte Carlo approach, as described in Section 2.1. For the exceedance probability levels listed in Table 4, the linear VBM value is determined using the Rayleigh distribution and the corresponding RCW is evaluated accordingly. Based on the assumption that the response at each exceedance probability level is primarily driven by the underlying wave excitation process, the experimentally measured VBM is treated as a re-evaluation of the response magnitude at that probability level.

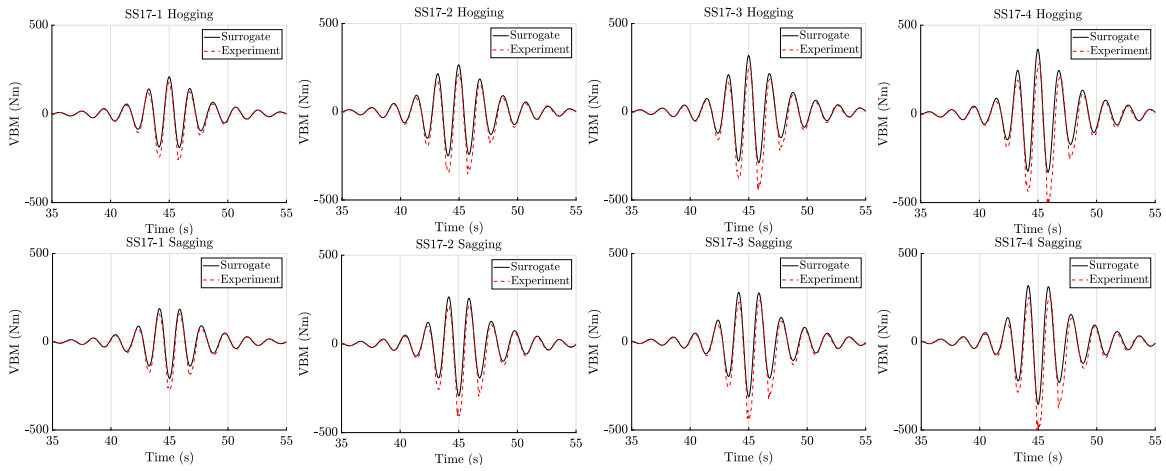

Fig. 9. Experimentally measured VBM responses for hogging (top row) and sagging (bottom row) for SS17.

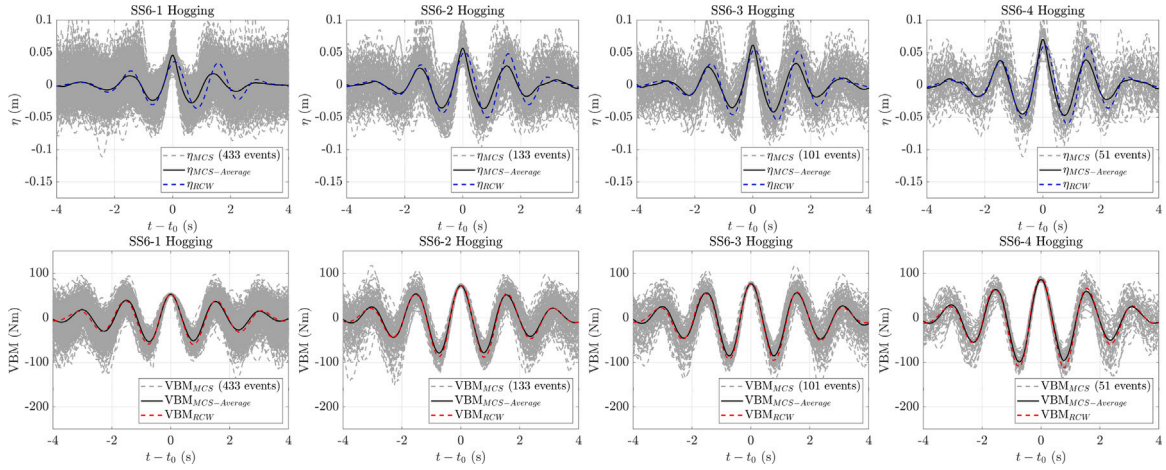

Fig. 10. Comparison between RCW and IW: Experimentally measured wave elevation profiles(top row) and VBM profiles (bottom row) for SS6-Hogging.

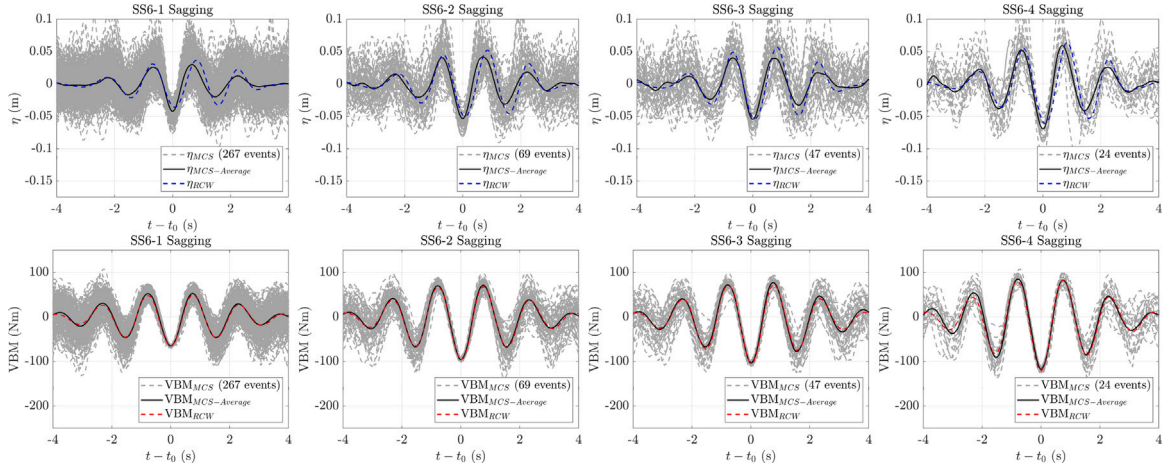

Fig. 11. Comparison between RCW and IW: Experimentally measured wave elevation profiles(top row) and VBM profiles (bottom row for SS6-Sagging).

The results of the procedure outlined above are presented in Fig. 14 for the five sea states. The ensemble VBM distribution obtained by the Monte Carlo approach is denoted as Exp. MCS and presented in blue colour. The Jeffrey 95 % confidence interval is also shown, to assess the statistical variability (Brown et al., 2001). Finally, the results of the design wave methodology for each exceedance probability level, are presented through the red-filled circles. It is shown that the RCW approach accurately captures the VBM distribution throughout all the sea states. Despite using the linear values of the symmetric Rayleigh distribution for the conditioning, the experimentally reproduced RCW-induced responses estimate very well the non-symmetric Monte Carlo distribution. Especially for hogging, there is an excellent agreement between the Monte Carlo and RCW results throughout the whole range

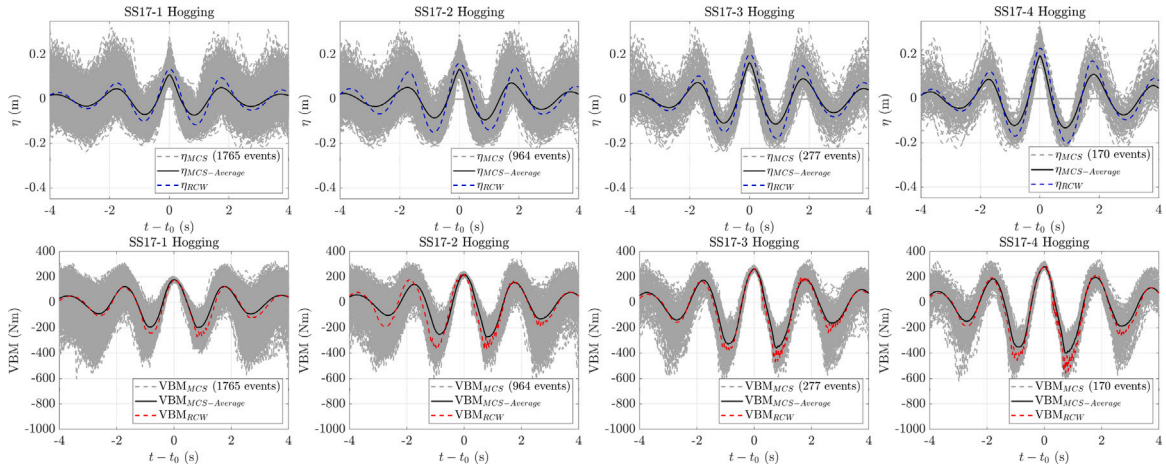

Fig. 12. Comparison between RCW and IW: Experimentally measured wave elevation profiles(top row) and VBM profiles (bottom row) for SS17-Hogging.

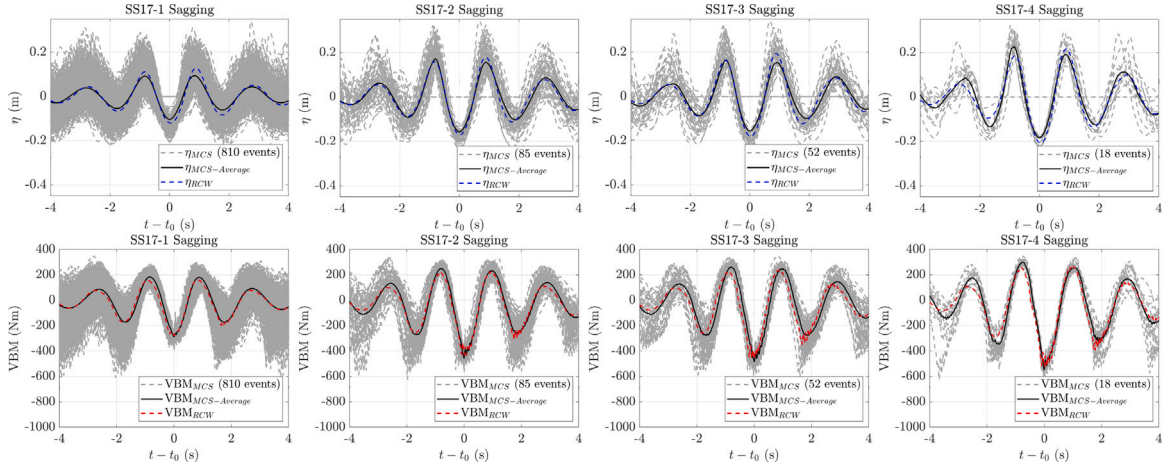

Fig. 13. Comparison between RCW and IW: Experimentally measured wave elevation profiles(top row) and VBM profiles (bottom row) for SS17-Sagging.

of sea states. In the case of sagging, the VBM is overall slightly underpredicted. However, the performance of the proposed approach does not deteriorate with the increase of the wave nonlinearity, which indicates that it can be applied even for very low probability events where the Monte Carlo method would be impractical. It is recalled here that for events with very low probability, the Monte Carlo approach would require a significantly increased duration, while with the design wave approach, there is always one single wave episode that needs to be tested.

Following the analysis of Kim et al. (2024a), the quantification of the degree of nonlinearity is made through the nonlinear factor of the VBM, defined as

$$f_{NL} = \frac{\mathrm{VBM}_{NL}}{\mathrm{VBM}_{L}} - 1 \tag{8}$$

where VBM_{L} denotes the linear response and VBM_{NL} denotes the VBM value for the same POE level, evaluated by the high-fidelity model. Similar to the irregular wave scenario, the nonlinear factor for the RCW can be devised as the ratio of the experimentally captured maximum VBM, to the corresponding linear value used for the conditioning.

Fig. 15 depicts the nonlinear factor for the five sea states in hogging and sagging conditions, with respect to the linear VBM values. For each sea state (corresponding to one colour), the continuous lines correspond to f_{NL} as calculated by the Monte Carlo distribution, and the filled circles correspond to the RCW results. The nonlinear factor exhibits similar behaviour for all sea states, implying that it is mostly influenced by the magnitude of the linear VBM and less by the difference in the environmental conditions (H_s and T_p). More specifically, in the case of hogging, the nonlinear effect is overall steady at approximately −15%, while in sagging a clear increasing trend is noticed in a much wider range from 10 to around 40%. Regarding the prediction of the nonlinear factor using the RCW, the variations with respect to the linear VBM values are captured very accurately throughout the whole range of sea states. In the case of sagging, there is a minor underprediction of less than 5% for every case, while in the case of hogging, the design wave methodology provides slightly conservative results.

In general, several sources of uncertainty can be identified throughout the experimental approach presented in this paper, contributing to differences between the Monte Carlo and the design wave results. First, provided that the moored containership exhibits some slow-drift motions, the position of encounter with the waves might deviate from the target position of $x_0 = 18.2$ m. In Kim (2022), the influence of the ship location for waves focused at x_0 has been investigated. It was found that when the containership was installed at a position 0.4 m from the default position, the difference in the measured extreme response was below 1%. Furthermore, even though reflections of the ship-generated wave field on the walls of the basin and the wavemaker can be neglected for the RCW tests, that is not the case for irregular waves.

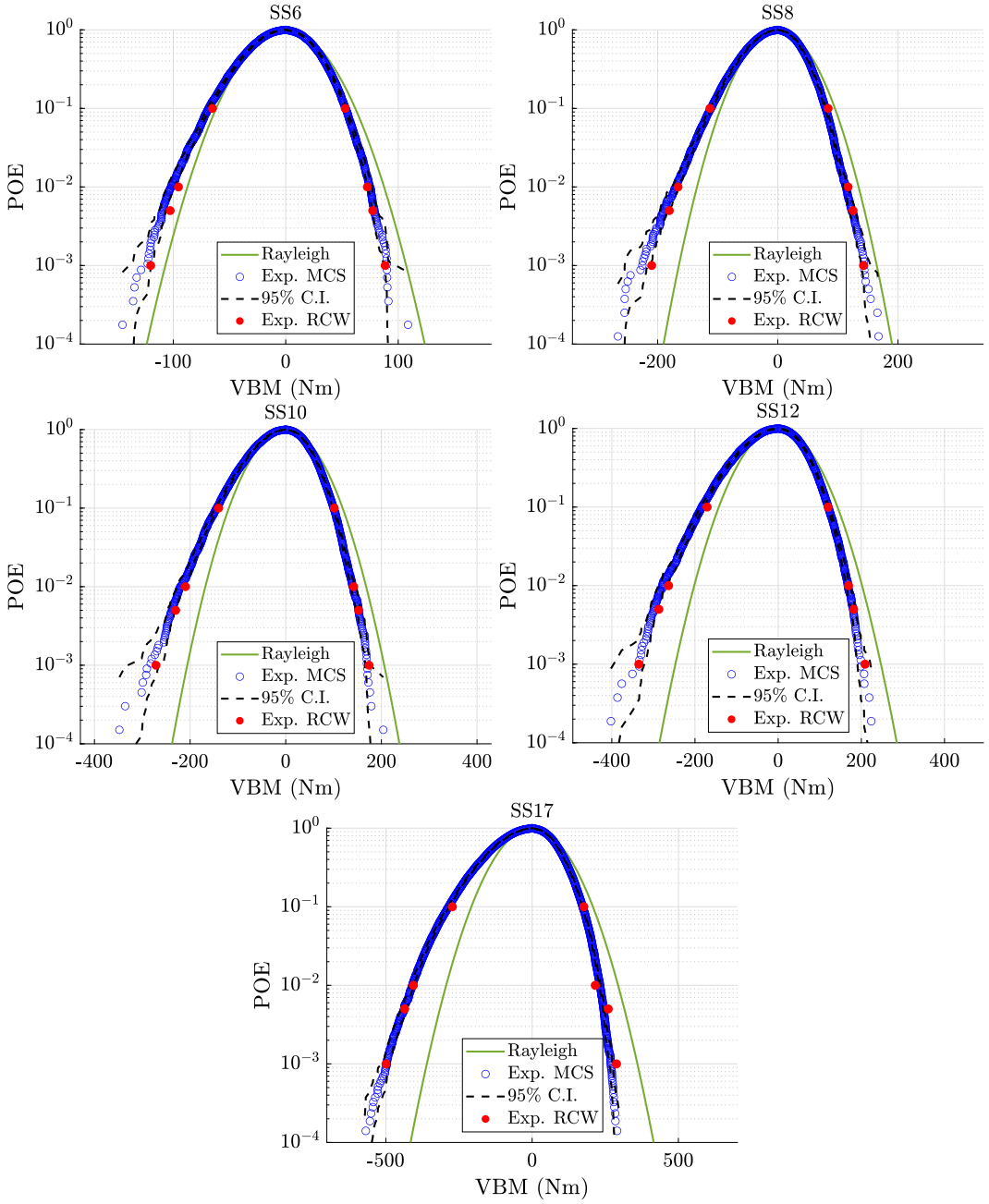

Fig. 14. Probability of exceedance curve for all sea states.

Regarding the limitations of the approach, it shall be emphasized that in the present study, an RAO-based surrogate model was used because the VBM is a response mostly driven by linear hydrodynamics and more specifically by the pressure distribution on the rigid hull. Therefore, a linear response model can successfully identify the wave episodes inducing extreme nonlinear events. However, if the flexibility of the hull is taken into account, hydroelastic effects will result in significant deterioration in the performance of the present approach (Drummen et al., 2009). Moreover, in the case of responses that are excited by resonant effects, outside the wave frequency range, such as the slow-drift motions of moored floating structures, the use of an RAO-based model will largely underpredict the extreme responses, as shown in Bouscasse et al. (2024) and Ripe and Lande-Sundall (2023). Towards this end, different and more accurate surrogate models need to be tested (Takami et al., 2020; Lim and Kim, 2018) which is also a direction for future work within the HOS-RCW approach.

5.2. Numerical investigation of design wave methodology

Finally, the applicability of the proposed methodology with CFD as the high-fidelity evaluation is demonstrated. The present section begins with the validation of the capacity of an in-house CFD solver to compute accurately the VBM of the containership during RCW events. At the same time, the numerical setup for RCW simulations is also investigated. The obtained response distribution for SS10 is then compared with the experimental RCW approach, as well as with the reference Monte Carlo distribution.

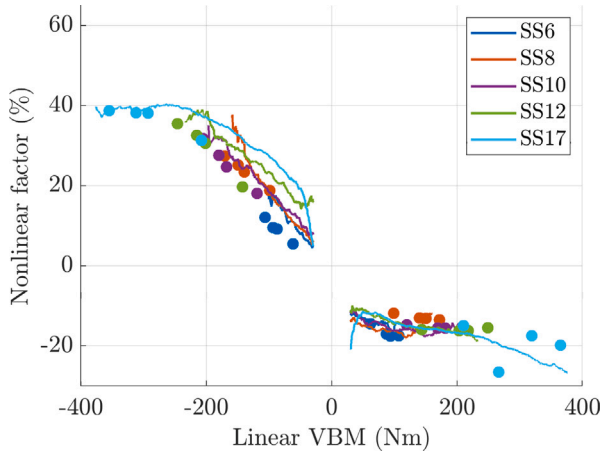

Fig. 15. Nonlinear factor with respect to linear VBM: IW (continuous line), design waves (filled circles).

Table 5
Numerical setups used for the convergence study.

Setup	Cells	Cells per λ_p	Cells per H_s	T_p/dt
M1	405k	84	5	100
M2	870k	130	8	150
M3	1270k	168	10	200
M4	5800k	168	20	400

5.2.1. Validation of in-house CFD solver

As a first step, a mesh and time step sensitivity study is presented for the numerical setups shown in Table 5. The numerical study was restricted to the SS10 cases and four different meshes with the same refinement zones but increasing resolution were built. For each mesh, the time step is chosen to keep a constant Courant number between the different setups. The SS10-3 case was chosen as the reference for the grid convergence, as it presents a large nonlinear factor. The results of the wave propagation for SS10-3 are shown in Fig. 16, where the accurate propagation of the wave episodes is confirmed for all setups. In the same Figure, the VBM is also plotted on the right column, for hogging and sagging conditions respectively. In Fig. 17, the associated heave and pitch motions are illustrated. It is emphasized that the VBM calculation requires both the correct propagation of the waves, as well as the capture of the body motions. The results show that the short duration of the test, starting as the wave impulse is already in the domain but not yet on the ship, is sufficient to ensure the waves and the motions are accurately reproduced. Small deviations from the experimental results are visible after the target time of 45 s. For simplifications, the surge is fixed during these simulations, which could be a possible explanation for these discrepancies.

To compare quantitatively the numerical and experimental results, two quantities are extracted: the relative error in the VBM extremum (maximum for hogging and minimum for sagging) attained during the CFD and the Improved Surface Similarity Parameter (ISSP) (Perlin and Bustamante, 2016; Kim et al., 2023a). The ISSP is a quantification of the resemblance of two time series and is defined as

$$\text{ISSP} = \frac{\left[\int \left|F_{num}(\omega) - F_{exp}(\omega)\right|^2 d\omega\right]^{1/2}}{\left(\int \left[\left|F_{num}(\omega) - \bar{F}_{exp}(\omega)\right| + \left|F_{exp}(\omega) - \bar{F}_{exp}(\omega)\right|\right]^2 d\omega\right)^{1/2}} \tag{9}$$

where F_{num} and F_{exp} are the complex Fourier coefficients of the examined and reference time series respectively and $\bar{F}_{exp}(\omega)$ is the frequency averaged experimental coefficient. An ISSP value equal to zero, implies totally overlapping time series, while an increase signifies deviation between the numerical and experimental results. The time interval taken into account for the computation of the ISSP has been set equal to the duration of the numerical simulation. The error of the extremum gives an insight into the actual nonlinear factor achieved by the CFD computation, which is the primary target of this study.

The two error quantification methods (ISSP and peak VBM error) are presented for the case SS10-3 as a function of the numerical setup M1 to M4 in Fig. 18. For both hogging and sagging, the discrepancy between numerical and experimental results decreases slowly and with some oscillations from M1 to M4. For this case, the results show that the solver and numerical methodology used are sufficient to correctly capture both the peak in VBM and the whole response time series. In the same Figure, the required CPU time is plotted for each setup M1 to M4 and a significant increase is observed. To perform the calculations on the other cases, the setup M2 is chosen, which combines a short computation time (less than 15 CPU hours to simulate 10 s of experiments) and sufficient accuracy.

5.2.2. Prediction of VBM distribution using CFD simulations

Having ensured that the CFD solver is capable of accurately and efficiently evaluating the VBM on the containership under RCW episodes, the second step of the methodology was implemented in a fully numerical framework. To this end, all HOS-RCW episodes that were derived for SS10 were reproduced in the CFD-based NWT and the obtained peak VBM was used to correct the response distribution, as shown in Fig. 19. Overall, the differences between the experimental and CFD design wave results are almost non-discernible, demonstrating the ability to transfer the high-fidelity evaluation step to a CFD-based NWT. Therefore, the full methodology can be implemented solely based on numerical calculations, from the definition of the RCW with a low-fidelity response model to the simulation of the RCW with a high-fidelity CFD solver at a quite reasonable computational cost.

6. Conclusions

In this paper, a multi-fidelity design wave methodology is presented for the assessment of the VBM response of a zero-speed containership. The proposed approach circumvents time-consuming irregular wave tests to obtain the fully nonlinear response distribution. It consists of two steps, which correspond to the use of wave–structure interaction models of different fidelity. First, an RAO-based response model is used to obtain a preliminary distribution of the response of interest. For certain probability levels, the equivalent response values are extracted and, together with the linear surrogate, they are used to determine the response-conditioned waves. The main novelty of this study is that within this surrogate, a fully nonlinear wave model is used that solves the wave propagation inside a numerical wave tank. Therefore, it overcomes the limitation of the response-conditioning techniques that provide linear wave sequences, which cannot be accurately reproduced in real conditions. The output of this first step is the wavemaker motion that will yield the nonlinear wave episode. Following, the second step of the methodology consists of the reproduction of those waves with high-fidelity tools (model tests or CFD) to obtain the fully nonlinear response to the calculated design wave and re-evaluate the response distribution.

An investigation of the reproducibility of the wave episodes, obtained by the proposed method, proves that they can be generated with very fine accuracy and without any limitation regarding the severity of the sea state. Moreover, the RCW wave elevation and RCW-induced responses are comparable with the ensemble of irregular wave events during which a ±5% VBM was measured, indicating the ability of the method to determine the most probable wave and response profile. Regarding the short-term probabilistic assessment of the VBM, the design wave results are compared against an experimental Monte Carlo approach in irregular waves and excellent agreement is found

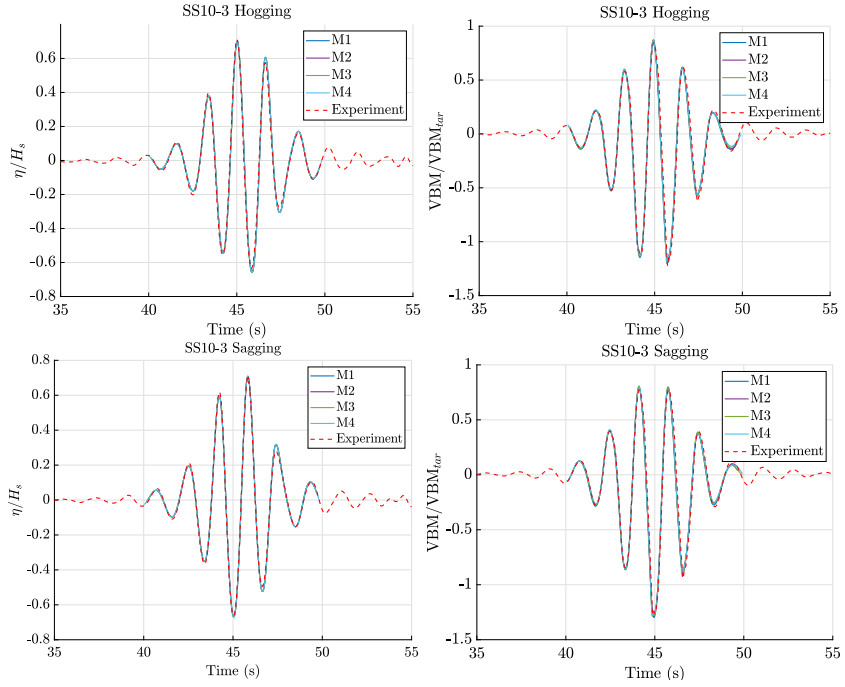

Fig. 16. Grid and timestep convergence study: Wave elevation (left column) and VBM (right column) for hogging and sagging case of SS10-3.

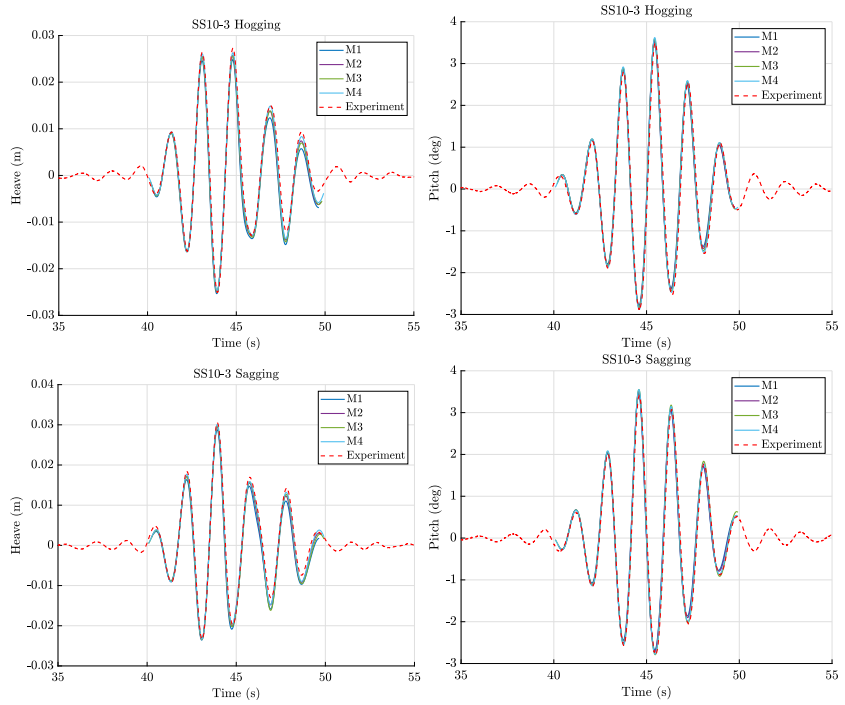

Fig. 17. Grid and timestep convergence study: Heave (left column) and pitch (right column) motions for hogging and sagging case of SS10-3.

for all sea states. To quantify the nonlinear effect of the response, the nonlinear factor is also investigated, defined as the ratio of the measured VBM to the linear VBM at each POE level. As also depicted in the case of the VBM distribution, the nonlinear factor in irregular waves can be well described by the design wave approach, despite some slight deviations.

Finally, the applicability of the design wave methodology is also demonstrated in a purely numerical framework using an OpenFOAM-based in-house CFD solver. The grid and timestep independence study shows excellent convergence properties and a highly efficient numerical setup is sought to perform simulations for each RCW episode. The short duration of the simulation and the absence of wave reflections,

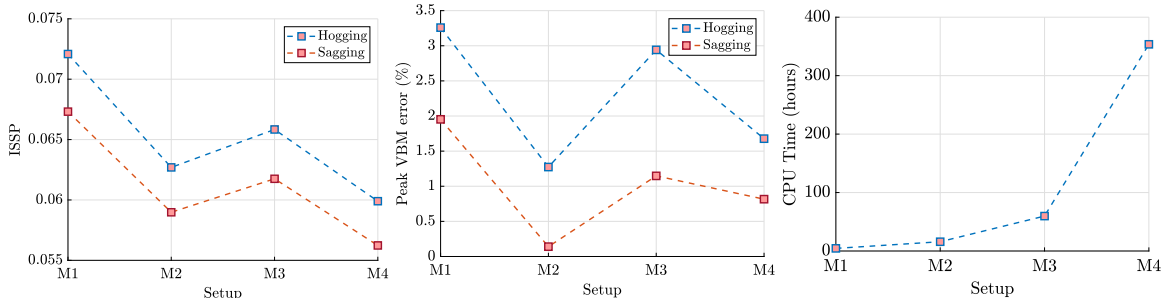

Fig. 18. SS10-3: ISSP (left), absolute peak differences (middle) and total CPU time (right) for each numerical setup.

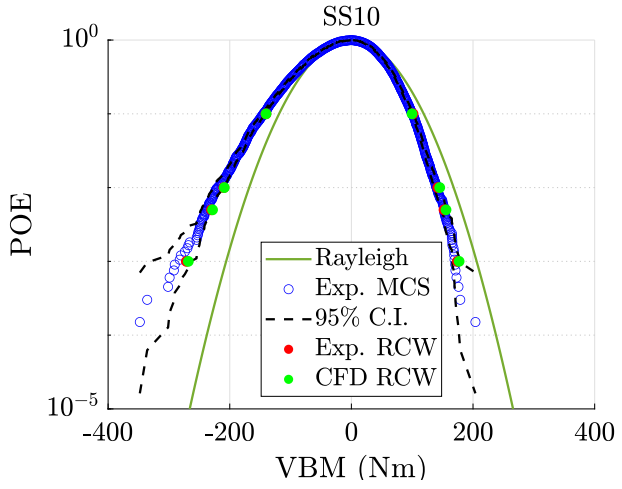

Fig. 19. Comparison between numerical and experimental evaluation of the exceedance probability with design waves for SS10.

allow the reduction of the size of the mesh and relaxation zones. Eventually, all the wave episodes of SS10 are simulated with that setup and the obtained results are compared against the experimental results. Excellent agreement is found in the prediction of the short-term extreme VBM distribution using CFD simulations, confirming that the full two-step methodology can be potentially applied with solely numerical means.

CRediT authorship contribution statement

Athanasios Dermatis: Writing – review & editing, Writing – original draft, Methodology, Investigation, Data curation, Conceptualization. **Marine Lasbleis:** Writing – review & editing, Writing – original draft, Software, Methodology, Data curation, Conceptualization. **Shinwoong Kim:** Methodology, Investigation, Conceptualization. **Guillaume De Hauteclocque:** Writing – review & editing, Validation, Supervision, Methodology, Investigation, Conceptualization. **Benjamin Bouscasse:** Writing – review & editing, Supervision, Methodology, Investigation, Data curation, Conceptualization. **Guillaume Ducrozet:** Writing – review & editing, Supervision, Methodology, Investigation, Conceptualization.

Declaration of competing interest

The authors declare that they have no known competing financial interests or personal relationships that could have appeared to influence the work reported in this paper.

Acknowledgement

The work presented in this paper was supported by Centrale Nantes - Bureau Veritas research chair and by the WASANO project, funded by the French National Research Agency (ANR) as part of the "Investissements d'Avenir" Programme (ANR-16-IDEX-0007).

References

Adegeest, L., Braathen, A., Vada, T., 1998. Evaluation of methods for estimation of extreme nonlinear ship responses based on numerical simulations and model tests. In: Proc. 22nd Symposium on Naval Hydrodynamics. Washington DC, pp. 70–84.

Alford, L.K., 2008. Estimating Extreme Responses using a Non-Uniform Phase Distribution (Ph.D. thesis). University of Michigan.

Aliyar, S., Ducrozet, G., Bouscasse, B., Sriram, V., Ferrant, P., 2022. Efficiency and accuracy of the domain and functional decomposition strategies for the wave-structure interaction problem. Ocean Eng. 266, 112568. http://dx.doi.org/10.1016/j.oceaneng.2022.112568.

Bouscasse, B., Dermatis, A., Ducrozet, G., de Hauteclocque, G., Lasbleis, M., 2024. Assessment of nonlinear loads and motions through response-conditioned waves: practical applications and limits. In: 43rd International Conference on Ocean, Offshore and Arctic Engineering. American Society of Mechanical Engineers.

Bouscasse, B., Merrien, A., Horel, B., De Hauteclocque, G., 2022. Experimental analysis of wave-induced vertical bending moment in steep regular waves. J. Fluids Struct. 111, 103547. http://dx.doi.org/10.1016/j.jfluidstructs.2022.103547.

Brown, L.D., Cai, T.T., DasGupta, A., 2001. Interval estimation for a binomial proportion. Statist. Sci. 16, 101–133.

Brown, S., Tosdevin, T., Jin, S., Hann, M., Simmonds, D., Greaves, D., 2023. On the selection of design waves for predicting extreme motions of a floating offshore wind turbine. Ocean Eng. 290, 116400. http://dx.doi.org/10.1016/j.oceaneng.2023.116400.

de Hauteclocque, G., Derbanne, Q., El-Gharbaoui, A., 2012. Comparison of Different Equivalent Design Waves With Spectral Analysis. American Society of Mechanical Engineers Digital Collection, pp. 353–361. http://dx.doi.org/10.1115/OMAE2012-83405.

Der Kiureghian, A., 2000. The geometry of random vibrations and solutions by FORM and SORM. Probab. Eng. Mech. 15, 81–90.

Derbanne, Q., Bigot, F., de Hauteclocque, G., 2012. Comparison of design wave approach and short term approach with increased wave height in the evaluation of whipping induced bending moment. In: ASME 2012 31st International Conference on Ocean, Offshore and Arctic Engineering, OMAE.

Dietz, J., 2004. Application of Conditional Waves As Critical Wave Episodes for Extreme Loads on Marine Structures (Ph.D. thesis). Technical University of Denmark.

Dommermuth, D.G., Yue, D.K., 1987. A high-order spectral method for the study of nonlinear gravity waves. J. Fluid Mech. 184, 267–288.

Drummen, I., Wu, M., Moan, T., 2009. Numerical and experimental investigations into the application of response conditioned waves for long-term nonlinear analyses. Mar. Struct. 22, 576–593.

Ducrozet, G., Bonnefoy, F., Le Touzé, D., Ferrant, P., 2012. A modified high-order spectral method for wavemaker modeling in a numerical wave tank. Eur. J. Mech. B Fluids 34, 19–34.

Ducrozet, G., Fink, M., Chabchoub, A., 2016. Time-reversal of nonlinear waves: applicability and limitations. Phys. Rev. Fluids 1, 054302.

Engsig-Karup, A., Bingham, H., Lindberg, O., 2009. An efficient flexible-order model for 3D nonlinear water waves. J. Comput. Phys. 228, 2100–2118. http://dx.doi.org/10.1016/j.jcp.2008.11.028.

Fernández, H., Sriram, V., Schimmels, S., Oumeraci, H., 2014. Extreme wave generation using self correcting method — revisited. Coast. Eng. 93, 15–31. http://dx.doi.org/10.1016/j.coastaleng.2014.07.003.

Friis-Hansen, P., Nielsen, L.P., 1995. On the new wave model for the kinematics of large ocean waves. In: Proceedings of the 14th International Conference on Offshore Mechanics and Arctic Engineering. Copenhagen, Denmark.

Ghadirian, A., Bredmose, H., 2019. Investigation of the effect of the bed slope on extreme waves using first order reliability method. Energy Procedia 67, 102627.
Hann, M., Greaves, D., Raby, A., Howey, B., 2018. Use of constrained focused waves to measure extreme loading of a taut moored floating wave energy converter. Ocean Eng. 148, 33–42. http://dx.doi.org/10.1016/j.oceaneng.2017.10.024.
Hirt, C.W., Nichols, B.D., 1981. Volume of fluid (VOF) method for the dynamics of free boundaries. J. Comput. Phys. 39, 201–225. http://dx.doi.org/10.1016/0021-9991(81)90145-5.
Jasak, H., 1996. Error Analysis and Estimation for the Finite Volume Method with Applications To Fluid Flow (Ph.D. thesis). Imperial College, University of London.
Jensen, J., 2011. Extreme value predictions using Monte Carlo simulations with artificially increased load spectrum. Probab. Eng. Mech. 26, 399–404. http://dx.doi.org/10.1016/j.probengmech.2010.09.001.
Jensen, J.J., Andersen, I.M.V., Seng, S., 2014. Stochastic procedures for extreme wave induced responses in flexible ships. Int. J. Naval Arch. Ocean Eng. 6, 1148–1159. http://dx.doi.org/10.2478/IJNAOE-2013-0236.
Jensen, J.J., Capul, J., 2006. Extreme response predictions for jack-up units in second order stochastic waves by FORM. Probab. Eng. Mech. 21, 330–337.
Jensen, J.J., hyuck Choi, J., Nielsen, U.D., 2017. Statistical prediction of parametric roll using FORM. Ocean Eng. 144, 235–242. http://dx.doi.org/10.1016/j.oceaneng.2017.08.029.
Jensen, J.J., Olsen, A.S., Mansour, A.E., 2011. Extreme wave and wind response predictions. Ocean Eng. 38, 2244–2253. http://dx.doi.org/10.1016/j.oceaneng.2011.10.003.
Jin, S., Brown, S.A., Tosdevin, T., Hann, M.R., Greaves, D.M., 2022. Laboratory investigation on short design wave extreme responses for floating hinged-raft wave energy converters. Front. Energy Res. 10, http://dx.doi.org/10.3389/fenrg.2022.1069108.
Kim, D., 2012. Design Loads Generator: Estimation of Extreme Environmental Loadings for Ship and Offshore Applications (Ph.D. thesis). The University of Michigan.
Kim, S., 2022. Experimental Study on Wave Bending Moments of a Zero-Speed Rigid Containership Model in Regular, Irregular, and Equivalent Design Waves (Ph.D. thesis). École Centrale de Nantes.
Kim, S., Bouscasse, B., Ducrozet, G., Canard, M., De Hauteclocque, G., Ouled Housseine, C., Ferrant, P., 2022. Numerical and experimental study of a FORM-based design wave applying the HOS-NWT nonlinear wave solver. Ocean Eng. 263, 112287. http://dx.doi.org/10.1016/j.oceaneng.2022.112287.
Kim, S., Bouscasse, B., Ducrozet, G., Delacroix, S., De Hauteclocque, G., Ferrant, P., 2023b. Experimental investigation on wave-induced bending moments of a 6 750-TEU containership in oblique waves. Ocean Eng. 284, 115161. http://dx.doi.org/10.1016/j.oceaneng.2023.115161.
Kim, Y.J., Canard, M., Bouscasse, B., Ducrozet, G., Le Touzé, D., Choi, Y.M., 2024b. High-order spectral irregular wave generation procedure in experimental and computational fluid dynamics numerical wave tanks, with application in a physical wave tank and in open-source field operation and manipulation. J. Marine Sci. Eng. 12, http://dx.doi.org/10.3390/jmse12020227.
Kim, S., De Hauteclocque, G., Bouscasse, B., Lasbleis, M., Ducrozet, G., 2024a. Experimental analysis of extreme wave loads on a containership. Ocean Eng. http://dx.doi.org/10.1016/j.oceaneng.2024.118031.
Kim, I.C., Ducrozet, G., Bonnefoy, F., Leroy, V., Perignon, Y., 2023a. Real-time phase-resolved ocean wave prediction in directional wave fields: Enhanced algorithm and experimental validation. Ocean Eng. 276, 114212.
Lim, D.H., Kim, Y., 2018. Design wave method for the extreme horizontal slow-drift motion of moored floating platforms. Appl. Ocean Res. 71, 48–58.
Mohamad, M., Sapsis, T., 2018. Sequential sampling strategy for extreme event statistics in nonlinear dynamical systems. Proc. Natl. Acad. Sci. 115, http://dx.doi.org/10.1073/pnas.1813263115.
Perlin, M., Bustamante, M.D., 2016. A robust quantitative comparison criterion of two signals based on the sobolev norm of their difference. J. Engrg. Math. 101, 115–124.
Quon, E., Platt, A., Yu, Y.H., Lawson, M., 2016. Application of the most likely extreme response method for wave energy converters. In: International Conference on Offshore Mechanics and Arctic Engineering. American Society of Mechanical Engineers, V006T09A022.
Ripe, A.M.T., Lande-Sundall, D., 2023. A comparison of extreme mooring loads and response of a spar-buoy wind turbine using conditional waves. J. Phys. Conf. Ser. 2626.
Santos, S., Matioli, L., Beck, A., 2012. New optimization algorithms for structural reliability analysis. CMES Comput. Model. Eng. Sci. 83, 23–55.
Schmittner, C., Kosleck, S., Hennig, J., 2009. A phase-amplitude iteration scheme for the optimization of deterministic wave sequences. In: International Conference on Offshore Mechanics and Arctic Engineering. pp. 653–660. http://dx.doi.org/10.1115/OMAE2009-80131.
Seiffert, B.R., Ducrozet, G., Bonnefoy, F., 2017. Simulation of breaking waves using the high-order spectral method with laboratory experiments: wave-breaking onset. Ocean Model. 119, 94–104.
Seng, S., Jensen, J.J., Malenica, Š., 2014. Global hydroelastic model for springing and whipping based on a free-surface CFD code (OpenFOAM). Int. J. Naval Arch. Ocean Eng. 6, 1024–1040. http://dx.doi.org/10.2478/IJNAOE-2013-0229.
Seyffert, H.C., 2018. Extreme Design Events Due To Combined, Non-Gaussian Loading (Ph.D. thesis). The University of Michigan.
Song, X., Wang, S., Hu, Z., Li, H., 2019. A hybrid Rayleigh and Weibull distribution model for the short-term motion response prediction of moored floating structures. Ocean Eng. 182, 126–136. http://dx.doi.org/10.1016/j.oceaneng.2019.04.059.
Takami, T., Fujimoto, W., Houtani, H., Matsui, S., 2023. Combination of HOSM and FORM for extreme wave-induced response prediction of a ship in nonlinear waves. Ocean Eng. 286, 115643.
Takami, T., Komoriyama, Y., Ando, T., Ozeki, S., Iijima, K., 2020. Efficient FORM-based extreme value prediction of nonlinear ship loads with an application of reduced-order model for coupled CFD and FEA. J. Marine Sci. Technol. 25, 327–345. http://dx.doi.org/10.1007/s00773-019-00667-8.
Torhaug, R., 1996. Extreme Response of Nonlinear Ocean Structures: Identification of Minimal Stochastic Wave Input for Time-Domain Simulation (Ph.D. thesis). Stanford University.
Tosdevin, T., Jin, S., Simmonds, D., Hann, M., Greaves, D., 2022. On the use of constrained focused waves for characteristic load prediction. In: Trends in Renewable Energies Offshore, first ed. CRC Press, London, pp. 609–617. http://dx.doi.org/10.1201/9781003360773-69.
Tromans, P.S., Anaturk, A.R., Hagemeijer, P., 1991. A new model for the kinematics of large ocean waves-application as a design wave. In: The First International Offshore and Polar Engineering Conference. OnePetro.
van Essen, S.M., Monroy, C., Shen, Z., Helder, J., Kim, D.H., Seng, S., Ge, Z., 2021. Screening wave conditions for the occurrence of green water events on sailing ships. Ocean Eng. 234, 109218.
van Essen, S.M., Scharnke, J., Seyffert, H.C., 2023. Required test durations for converged short-term wave and impact extreme value statistics — part 1: Ferry dataset. Mar. Struct. 90, 103410. http://dx.doi.org/10.1016/j.marstruc.2023.103410.
van Essen, S., Seyffert, H., 2023. Finding dangerous waves—Review of methods to obtain wave impact design loads for marine structures. J. Offshore Mech. Arct. Eng. 145, 060801. http://dx.doi.org/10.1115/1.4056888.
West, B.J., Brueckner, K.A., Janda, R.S., Milder, D.M., Milton, R.L., 1987. A new numerical method for surface hydrodynamics. J. Geophys. Res.: Oceans 92, 11803–11824.